Molecular Dynamic Simulation of Fracture and Effect of Hydrogen on Fracture of Tungsten at High Temperature*

高温下钨断裂及氢影响钨断裂的分子动力学模拟

OUYANG Yi-fang, CHEN Hong-mei, ZHONG Xia-ping
欧阳义芳, 陈红梅, 钟夏平

(College of Physics Science and Technology, Guangxi University, Nanning, Guangxi, 530004, China)
(广西大学物理科学与工程技术学院, 广西南宁 530004)

Abstract: The fracture of Tungsten single crystal has been investigated under uniaxial strain at temperature 1000 K. The results indicate that the {100} plane cleaves more easily than the {110} plane. The cleavage of the {100} plane depends on the orientation of the crack-tip. The result is in good agreement with the experiment at low temperature. The simulation for the fracture of the $(\bar{1}10)<111>$ indicates that the fracture mechanism is not cleavage. Two cases of shear strain are also studied. The present results are also coincident with available experiments of room temperature. The present results indicate that the fracture of Tungsten at high temperature is similar to that at low temperature. The effect of Hydrogen on the fracture is also discussed. It can affect the front of the crack-tip and decrease the yield stress.

Key words: molecular dynamic simulation, Tungsten, fracture, embedded atom method

摘要: 用分子动力学模拟在 1000K 温度下单晶钨在单轴应变的情形下断裂和氢对钨断裂的影响。结果表明: {100}面的辟裂比{110}面要容易。{100}面的辟裂与裂纹尖端的取向有关, 模拟结果与低温下的实验结果符合得比较好。$\{\bar{1}10\}$面<111>方向的断裂不是辟裂方式。切应变的模拟结果也与实验相符。氢的加入对裂纹尖端影响比较大, 能显著降低应力。

关键词: 分子动力学 钨 断裂 嵌入原子理论
中图法分类号: TG113.25 **文献标识码**: A **文章编号**: 1005-9164(2006)03-0212-05

1 Introduction

The deformation characteristics of the body central cubic (bcc) metals differ from the face central cubic (fcc) metals. The yield strength and flow stress of bcc metals increase rapidly with the decreasing of temperature and the increasing of strain rate. The mechanical behavior and fracture of bcc metals have been widely studied. However, the investigations focus on Iron[1,2]. For Tungsten, which is a very important refractory metal, fewer works have been done. Some experimental information has been obtained, eg Riedle et al[3,4]. found the cleavage anisotropy of Tungsten single crystals and concluded that this might be the consequence of anisotropic lattice trapping. Kogayashi et al[5]. studied the crack propagation and the plastic zone of crack-tip in Tungsten. Chiem et al[6]. studied the plastic deformation under shear loading. Kohlhoff et al[7]. simulated the crack propagation in single crystal Tungsten using the method combined finite-

收稿日期: 2005-10-12
修回日期: 2005-12-01
作者简介: 欧阳义芳(1965-), 男, 湖南衡东人, 教授, 主要从事凝聚态物理研究。
* Supported by National Natural Science Foundation of China (No. 10264001)。

element and atomistic model at room and low temperatures. These results are in agreement with experiments. There are some efforts[8,9] applied to understand the effects of Hydrogen on the fracture of metals.

In this paper, the fracture of Tungsten single crystal is simulated with atomistic model at high temperature. The effect of Hydrogen on fracture process is also discussed.

2 The potential and the atomistic model

2.1 The interaction potential of Tungsten and Hydrogen

In the molecular dynamic simulation, a more important argument is about the inter-atomic potential. Several potentials have been presented for Tungsten[10,11]. In this simulation, the potential based on the embedded atom method (EAM)[12] is used.

According to the scheme of EAM, the energy of an atom can be described as[11]

$$E_i(r) = F_i(\rho_i) + \frac{1}{2}\sum_{j(\neq i)}\phi(r_{ij}) \tag{1}$$

with

$$\rho_i = \sum_{j(\neq i)} f(r_{ij}); \tag{2}$$

$$f(r) = f_e\exp[-\beta(\frac{r}{r_1} - 1)]. \tag{3}$$

The effective pair potential between atoms and the embedding function are taken as

$$\phi(r) = k_0 + k_1(\frac{r}{r_1})^2 + k_2(\frac{r}{r_1})^4 + k_3(\frac{r_1}{r})^{12}; \tag{4}$$

$$F(\rho) = -F_0[1 - n\ln(\frac{\rho}{\rho_e})](\frac{\rho}{\rho_e})^n, \tag{5}$$

where r_1 indicates the distance of the first neighbour atom at equilibrium. The other arguments are the model parameters which can be determined by fitting the lattice constant, monovacancy formation energy, cohesion energy and elastic constants of Tungsten[11].

For Hydrogen, which is different from solid state metal elements, a few experimental data are available. So, the determination procedure of potential for Hydrogen is different from that of Tungsten. The Equation (1) is fitted to the equation of Rose et al[13]. for Hydrogen molecule.

$$E(r) = -E_C[1 + \alpha(\frac{r}{r_1} - 1)]\exp[-\alpha(\frac{r}{r_1} - 1)]. \tag{6}$$

And the embedding function is determined by fitting Equation (5) to the results obtained by Painter et al[14]. from the first principles. Combining Equation (1) and Equation (5), the effective pair potential can be written as followings

$$\phi(r) = -2E_C[1 + \alpha(\frac{r}{r_1} - 1)]\exp[-\alpha(\frac{r}{r_1} - 1)] + 2F_0[1 + n\beta(\frac{r}{r_1} - 1)]\exp[-n\beta(\frac{r}{r_1} - 1)]. \tag{7}$$

The interaction potential between Tungsten atom and Hydrogen atom is the same as that proposed by Johnson et al.[15].

$$\phi^{ab}(r) = \frac{1}{2}[\frac{f^b(r)}{f^a(r)}\phi^{aa}(r) + \frac{f^a(r)}{f^b(r)}\phi^{bb}(r)]. \tag{8}$$

Where superscripts a and b represent the Tungsten atom and Hydrogen atom respectively. The atomic electron density distribution function Equation (3) is fitted to the results of Clementi et al[16]. The potential between two atoms of W-W, H-H and W-H are demonstrated in Fig. 1. The functions of $f(r)$ and $\phi(r)$ are cut off by the following function in the range between r_{c1} and r_{c2}.

$$\phi_c(r) = \phi_e\exp[\gamma(\frac{r}{r_{c1}} - 1)(\frac{r}{r_{c2}} - 1)^{-1}]. \tag{9}$$

The functions and cutoff functions are combined at the point of $r = r_{c1}$ smoothly. The interatomic potentials for the atoms studied are shown in Fig. 1.

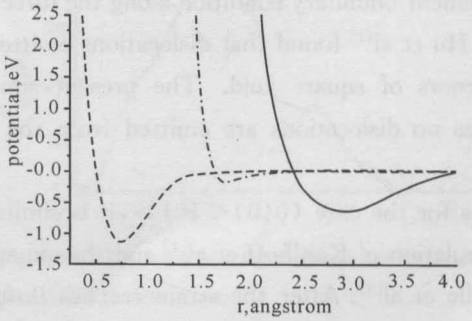

Fig. 1 The interatomic potentials of interaction between different atoms

——:W;----:H;— · — · —:W-H

2.2 The atomistic model in Molecular Dynamics

Hu et al[1] presented an atomistic model to simulate the deformation and fracture of single Iron. They concluded that the model size affected only the threshold value of stress at which the associated deformation mechanism activated or inactivated, but not the deformation mechanism for a given crystal orientation and boundary condition. The distributions of stress-strain curves are identical for different model

sizes. So, the similar scheme is used in this paper to simulate the fracture of Tungsten under uni-axial tensile and shear strain. The two ends of the cell are strained at a fixed rate and the stress is calculated. The x and z directions are used at periodic boundary condition and the y direction is used at displacement boundary condition. The simulations are performed at 1000 K. Time step: $\Delta t = 1$ fs. The total steps: 100000 steps; The cell size: $100 * 100 * 5 = 50000$ atoms. The force was applied by displacing the five layers of atoms on the top and the bottom of the cell according to the way of deformation. The deformation rate is 0.1% per 50 steps.

3 The results and discussion

3.1 Tensile

3.1.1 The brittle cleavage of the {100} planes

The {100} plane is notched at two different directions, i.e. (010)<100> and (010)<101> systems. The strains are applied along the <010> direction. The crack propagation deflects firstly to the direction <110>. This is in good agreement with those of experiment[4] and simulation[7] at room temperature. However, it refracts back after longer time simulation. This may be the consequence of the displacement boundary condition along the direction <010>. Hu et al[1] found that dislocations emitted from the corners of square void. The present simulation indicates no dislocations are emitted from the crack-tip.

As for the case (010)<101>, it is similar with the simulation of Kohlhoff et al[7] and the experiments of Riedle et al[4]. After the strain reaches 0.054, the crack begins to propagate. For bcc Iron single crystal without the crack, the simulation of Hu et al[1] indicates that the deformation mechanism is twinning. The present simulation for Tungsten with crack indicates only the cleavage.

For the {010} crack system, the stress-strain curves for the cases mentioned above are given in Fig. 2. The stress may be too large in magnitude. However, from Figure 2, we can see that the yield stress is more different at these two directions. This tendency indicates that the cleavage comes out along the <101> direction more easily than along the <100>. Kohlhoff et al[7] calculated the stress intensity K_I of Tungsten at low temperature. They found that the stress intensity of the <100> is greater than that of the <101>. From the above discussion, the cleavage of the plane {100} is orientation dependence.

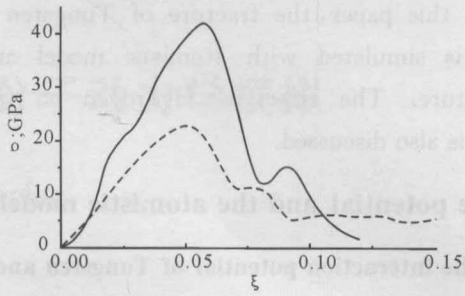

Fig. 2 The calculated stress-strain curves for crack of the {010} plane under different orientation of crack-tip
——: (010)[100]; ----: (010)[101]

3.1.2 The crack of the plane {110}

For the {110} plane cleavage, three cases are studied. The simulation for the case (101)<010> indicates that the crack extend straightly. This is as same as the results of Kohlhoff et al[7]. The present simulation for $(1\ \bar{1}\ 0)<110>$ agrees well with the experiment. The crack-tip changes direction to the <100>. However, the results of Kohlhoff et al[7] indicate the crack propagates straightly. No dislocations appears, Hu et al[1] found that two slip bands developed under the periodic boundary condition for perfect iron crystal.

For crack system $(\bar{1}\ 10)<111>$, the results indicate that some microvoids are produced in front of the crack-tip. The crack propagation of the case shows that the features and characteristics of microvoid formation and coalescence. The mechanism of fracture in this case is different from that at other two orientations. The similar results are obtained by Hu et al[1] for perfect iron crystal under the same condition.

The stress-strain curves in these three cases are given in Fig. 3. It indicates that the $(1\ \bar{1}\ 0)<110>$ system is easier than the others. This conclusion is coincident with that of Kohlhoff et al[7].

Comparing to Fig. 2 and Fig. 3, it is clear that the cleavage of the (100) planes is the easy cleave planes. As pointed out by Riedle et al[3], the cleavage anisotropy may be interpreted only by the atomistic nature of the crystal, but not by the continuum elastic mechanics.

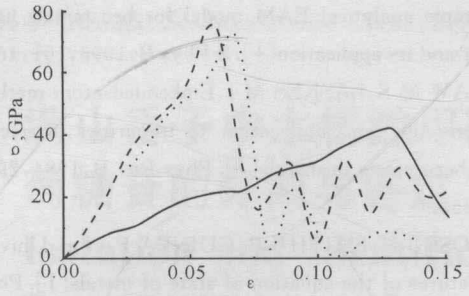

Fig. 3 The stress-strain curves for crack system {110} at different orientations under tensile strain

----:[101-010]; —— :[1 $\bar{1}$0-110]; ·····:[1 $\bar{1}$0-111]

3.2 Shear

Many works have been done for bcc metal under shear strain with the atomistic model simulation[17]. However, to our knowledge, no simulations have been done for Tungsten, especially at high temperature. Chiem et al[6] studied the plastic deformation of (1 $\bar{1}$0) and ($\bar{1}\bar{1}$2) planes at room temperature. The results indicate that the deformation mechanism for crack system (1 $\bar{1}$0)<111> is dislocation and ($\bar{1}\bar{1}$2)<111> is twinning. We use the present model to model this procedure. The present simulation indicates the deformation mechanism at high temperature is also the same as that at low temperature.

3.3 The effects of Hydrogen on the fracture

The mechanical properties of a lot of crystalline materials are affected by the presence of Hydrogen. In many cases, the application of the materials is nearly presented in the Hydrogen atmosphere. It is important to understand the effects of Hydrogen on the fracture. Many mechanisms[18,19] have been proposed for hydrogen embrittlement. It is well known that Hydrogen embrittlement is that Hydrogen dissolves into the interstitial sites of the crystal lattice and causes crack nucleation and growth in many metals under tensile stress[20]. From the binary diagram of W-H system[21], the solubility of Hydrogen in Tungsten is very little. The solution enthalpy of Hydrogen in Tungsten has been calculated using the above EAM potential. The value is $\Delta H = 0.3167$ eV/atom for Hydrogen solving in the central position of tetrahedron. The activation energy of Hydrogen diffusion in Tungsten has also been calculated without relaxation. The calculated activation enthalpy of diffusion, 0.364eV/atom, is in good agreement with the experiment[22]. There is no evidence of intermetallic compound in this system from the phase diagram. So we study the effects of Hydrogen on the fracture of Tungsten when the Hydrogen solve in the tetrahedral interstitial sites ahead of the fracture of crack-tip.

The occupations of Hydrogen at the interstitial sites are randomly and the composition of Hydrogen is about 0.5%. The interaction potential, given in Fig. 1, can give a positive enthalpy of solution for Hydrogen in Tungsten. This is the consequence of low solubility limitation of Hydrogen in Tungsten.

The present simulation indicates that crack-tip has not propagated in the crystal with Hydrogen when the strain reaches 0.072. However, the crack-tip has been progressed into crystal without Hydrogen under the same strain. After the strain reaches 0.081, the crack propagates forward. The crack-tip in the crystal with Hydrogen becomes blunt. It indicates that the Hydrogen can blunt the crack-tip. The simulation also indicates that the Hydrogen atoms segregate. Fig. 4 gives the stress-strain curves with and without Hydrogen. From Fig. 4, one can see that the Hydrogen can decrease the strength largely and the distribution is different from that without Hydrogen.

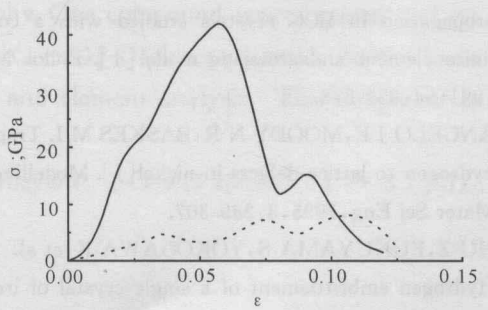

Fig. 4 The stress-strain curves with and without Hydrogen under tensile strain

—— :without H; ----:with H

4 Conclusions

The fracture of single Tungsten with and without Hydrogen under tensile and shear strain have been studied with Molecular Dynamics. The cleavage of the {100} plane is depended on the orientation of the crack-tip. The cleavage of the plane {100} is more easily than that of the plane {110}. The fracture mechanism of crack system ($\bar{1}$ 10) < 111 > is microvoid formation and coalescence. The deformation for (1 $\bar{1}$0)<111> and ($\bar{1}\bar{1}$2)<111> systems are

different under shear strain. The former is dislocation emission and the latter is twinning. The effect of Hydrogen on the fracture of Tungsten results in bluntness of the crack-tip and decreasing of the yield stress.

References:

[1] HU S Y,LUDWIG M,KIZLER P,et al. Atomistic simulations of deformation and fracture of α-Fe [J]. Modelling Simul Mater Sci Eng,1998,6:567-586.

[2] CHEUNG K S,YIP S. A molecular-dynamics simulation of crack-tip extension: the brittle-to-ductile transition [J]. Modelling Simul Mater Sci Eng,1994,2:865-892.

[3] RIEDLE J,GUMBSCH P,FISCHMEISTER H F. Cleavage anisotropy in tungsten single crystals[J]. Phys Rev Lett,1996,76:3594-3597.

[4] RIEDLE J,GUMBSCH P,FISCHMEISTER H F,et al. Fracture studies of tungsten single crystals [J]. Mater Lett,1994,20:311-317.

[5] KOBAYASHI S,OHR S M. In situ fracture experiments in bbc metals[J]. Philos Mag A,1980,42:763-772.

[6] CHIEM C Y,LEE W S. The influence of dynamic shear loading on plastic deformation and microstructure of tungsten single crystals[J]. Mater Sci Eng:A,1994,186:43-50.

[7] RIEDLE J,GUMBSCH P,FISCHMEISTER H F. Crack propagation in BCC crystals studied with a combined finite element and atomistic model [J]. Philos Mag A,1991,64:851-878.

[8] ANGELO J E,MOODY N R,BASKES M I. Trapping of hydrogen to lattice defects in nickel[J]. Modelling Simul Mater Sci Eng,1995,3:289-307.

[9] HU Z,FUKUYAMA S,YOKOGAWA K,et al. Hydrogen embrittlement of a single crystal of iron on a nanometre scale at a crack tip by molecular dynamics[J]. Modelling Simul Mater Sci Eng,1999,7:541-551.

[10] BASKES M I. Modified embedded-atom potentials for cubic materials and impurities[J]. Phys Rev B,1992,46:2727-2742.

[11] OUYANG Y F,ZHANG B W,LIAO S Z,et al,A simple analytical EAM model for bcc metals including Cr and its application[J]. Z Phys B,1996,101:161-168.

[12] DAW M S,BASKES M I,Embedded-atom method: derivation and application to impurities, surfaces, and other defects in metals[J]. Phys Rev B,1984,29:6443-6453.

[13] ROSE J H,SMITH J R,GUINEA F,et al. Universal features of the equation of state of metals[J]. Phys Rev B,1984,29:2963-2969.

[14] PUSKA M J,NIEMINEN R M. Atoms embedded in an electron gas:immersion energies[J]. Phys Rev B,1981,24:3037-3047.

[15] JOHNSON R A. Alloy models with the embedded-atom method[J]. Phys Rev B,1989,39:12554-12559.

[16] CLEMENTI E,ROETTI C. Roothaan-Hartree-Fock atomic wavefunctions [J]. Atomic Data and Nuclear Data Tables,1974,14(3-4):179-232.

[17] TANG Q H,WANG T C. Correlative reference model and molecular dynamics simulation of dislocation emission process[J]. Comput Mater Sci,1998,12:73-83.

[18] GERBERICH W W,MARSH P,HOEHN J,et al. Crack growth from internal hydrogen-Temperature and microstructural effects in 4340 steel:Proceedings of the Corrosion-deformation Interactions [C]. Paris: Les Editions de Physique,1993:633-638.

[19] BRINBAUM H K. Mechanisms of Hydrogen-Related Fracture of Metals[M]//MOODY N R,THOMPSON A W. Hydrogen effects on material behavior. Warrendale PA:TMS,1990:693-697.

[20] SHEWMON P G. Grain boundary cracking[J]. Metall Mater Trans A,1998,29:1535-1544.

[21] MARTIENSSEN W. Landolt-Bornstein,phase equilibria, crystallographic and thermodynamic data of binary alloys,IV/5F[M]. Berlin:Springer,1996:270.

[22] FRAUENFELDER R. Solution and diffusion of hydrogen in tungsten[J]. J Vac Sci Technol,1969,6:388-397.

(责任编辑:蒋汉明　凌汉恩)